American Mineralogist, Volume 79, pages 1032–1041, 1994

The structure of high-pressure $C2/c$ ferrosilite and crystal chemistry of high-pressure $C2/c$ pyroxenes

D. A. HUGH-JONES
Research School of Geological and Geophysical Sciences, University College London, Gower Street, London WC1E 6BT, U.K.
A. B. WOODLAND
Bayerisches Geoinstitut, Universität Bayreuth, D-95440 Bayreuth, Germany
R. J. ANGEL*
Research School of Geological and Geophysical Sciences, University College London, Gower Street, London WC1E 6BT, U.K.

ABSTRACT

Single-crystal X-ray diffraction experiments in a diamond-anvil pressure cell have demonstrated that clinoferrosilite ($FeSiO_3$) with space group $P2_1/c$ transforms to a pyroxene with space group $C2/c$ at high pressure. The transformation has been reversed at room temperature and pressures between 1.48 and 1.75 GPa; it is first-order in character and is accompanied by a 3% decrease in the volume of the unit cell. The structure of this $C2/c$ polymorph has been refined from diffraction data collected at 1.87 GPa and contains a single, symmetrically distinct silicate tetrahedral chain, with a mean Si-O bond length of 1.63 Å and a chain extension angle (O3-O3-O3) of 138.4 ± 0.9°. The M1 and M2 cation sites are octahedrally coordinated, with mean bond lengths of 2.14 and 2.18 Å, respectively. This clinopyroxene is the Fe analogue of the $C2/c$ phase found in $MgSiO_3$ at pressures above 7 GPa.

The high-pressure $C2/c$ structure of ferrosilite differs considerably from the $C2/c$ phase found at elevated temperatures, with a β angle some 7° smaller and a silicate chain significantly more kinked than in the high-temperature form. It is also substantially different from $C2/c$ structures that contain Ca but is very similar (in terms of the sizes and distortions of the cation sites) to orthorhombic ferrosilite. The same structural relationships hold for the $MgSiO_3$ phases with $C2/c$ symmetry. The chemical behavior of these $C2/c$ forms of both $MgSiO_3$ and $FeSiO_3$ is therefore expected to resemble that of the corresponding orthopyroxenes.

INTRODUCTION

Pyroxenes make up almost 25% by volume of some mineralogical models of the Earth's upper mantle (Ringwood, 1975). The structure of the Ca-poor pyroxene has always been considered to be an orthopyroxene, although evidence for the stability at high pressures of a Ca-poor clinopyroxene has been available for some 15 yr (e.g., Yamamoto and Akimoto, 1977; Akaogi and Akimoto, 1977). Recent petrological experiments on the $MgSiO_3$ system in the pressure-temperature range 7–10 GPa and 900–1700 °C (Pacalo and Gasparik, 1990; Kanzaki, 1991) in combination with in-situ single-crystal diffraction experiments to 8 GPa at room temperature (Angel et al., 1992a) have confirmed the true stability of a high-pressure clinopyroxene phase with $C2/c$ symmetry. Orthoenstatite of composition $MgSiO_3$ transforms to this high-pressure clinoenstatite structure at the pressures and temperatures corresponding to a depth of 200–300 km within the Earth's upper mantle. Unlike other transformations between pyroxene polymorphs (e.g., Gasparik, 1990, and references therein), the orthoenstatite to high-pressure clinoenstatite transition involves substantial changes in the thermodynamic properties of the pyroxene; for example, the volume change at high pressure is some 3% (Angel and Hugh-Jones, 1994), and ΔS and ΔH are substantial fractions of the values associated with the higher-pressure breakdown reactions of pyroxene to either garnet or wadsleyite + stishovite (Angel and Hugh-Jones, 1994).

Further experimental work has suggested that the addition of small amounts of Ca or Al to the $MgSiO_3$ end-member has only a minor effect on the position of the orthopyroxene to high-pressure clinopyroxene phase boundary (Herzberg and Gasparik, 1991). However, since Fe is likely to be the largest substituent for Mg in orthopyroxenes, we are undertaking a study of the phase stabilities and properties of pyroxenes with composition $FeSiO_3$ to provide end-member data for the subsequent examination of the effect of Fe on the phase relations of

* Present address: Bayerisches Geoinstitut, Universität Bayreuth, D-95440 Bayreuth, Germany.

0003–004X/94/1112–1032$02.00

Ca-free pyroxenes. The form of the phase diagram of $FeSiO_3$ (ignoring the low-pressure breakdown to fayalite + quartz and the existence of a structurally distinct $C2/c$ phase stable at high temperatures) that can be deduced from experiments quenched from high pressures and temperatures is shown in Figure 1a. At pressures below 4 GPa, Lindsley (1965) reversed a phase boundary between orthoferrosilite and clinoferrosilite with space group $P2_1/c$, whereas Akimoto et al. (1965) reported the recovery of the same $P2_1/c$ clinoferrosilite phase from experiments that would lie in the stability field of orthoferrosilite if the boundary of Lindsley were extrapolated to higher pressures (Fig. 1a). One possible solution to this apparent discrepancy is for the phase diagram of $FeSiO_3$ to have the same topology as that of $MgSiO_3$, with a stability field for a $C2/c$ ferrosilite phase at high pressures (Fig. 1b). By analogy with $MgSiO_3$, this phase is expected to revert to $P2_1/c$ clinoferrosilite upon pressure release.

We have therefore undertaken an in-situ high-pressure single-crystal X-ray diffraction study of $P2_1/c$ clinoferrosilite and show that it transforms to a $C2/c$ phase at high pressures, whose structure we have determined. The crystal chemistry of the high-pressure $C2/c$ phases of both end-member compositions that are now known are compared in some detail with other pyroxene polymorphs of the same compositions to yield insights into the nature of the pyroxene phase diagram at high pressures and temperatures and to deduce the effect that the inversion of orthopyroxene to high-pressure clinopyroxene has on the distribution of trace elements between the pyroxene and other phases in the Earth's upper mantle.

Experimental details

Clinoferrosilite was synthesized at 8.0 GPa and 1200 °C in a multianvil press at the Bayerisches Geoinstitut. The sample assembly and experimental details are essentially the same as reported in Woodland and O'Neill (1993). The starting material was a mixture of fayalite and quartz, along with 5% by weight BaO-B_2O_3 as a flux (78 wt% BaO, 22 wt% B_2O_3). A slight excess of quartz was added to compensate for the dissolution of SiO_2 into the flux. Ag was used as the capsule material to prevent the loss of Fe to the capsule during the experiment. The duration of the experiment at pressure and temperature was 10.5 h.

A small crystal (measuring 60 × 30 × 20 μm) was selected from the sample of synthetic clinoferrosilite on the basis of its optical quality and large size, relative to the rest of the $FeSiO_3$ crystals in the sample. The compositions of several crystals from this sample were analyzed using energy-dispersive X-ray analysis with a Phillips CM20 FEG transmission electron microscope (at the Bayerisches Geoinstitut), which detected the presence of just Fe, Si, and O, indicating that the synthetic clinoferrosilite contained no impurities. Mössbauer experiments on the clinoferrosilite crystals (McCammon, personal communication) displayed no peaks attributed to Fe^{3+}, implying that the concentration of Fe^{3+} in the sample was

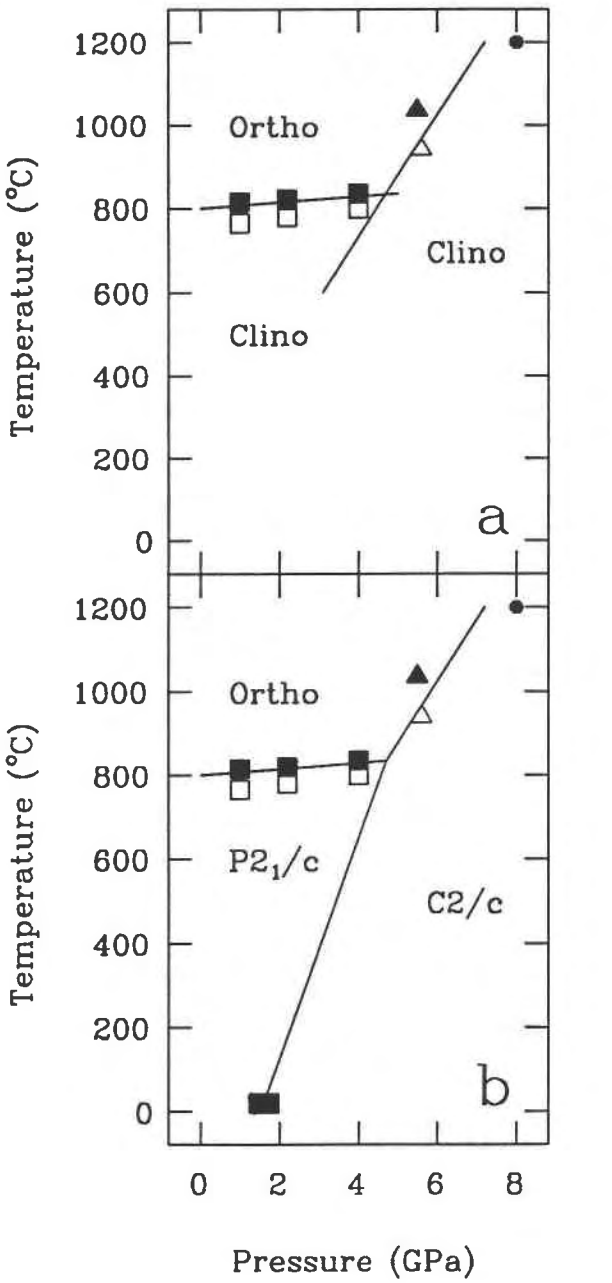

Fig. 1. (**a**) The ortho-clino $FeSiO_3$ phase boundaries of Lindsley (1965) and Akimoto et al. (1965). The pressures and temperatures of Lindsley's reversals are represented by squares. Only one reversal of the boundary was obtained by Akimoto et al. (shown by the triangles); the position of the phase boundary was constrained by several synthesis experiments on either side of it. The pressure and temperature at which our clinoferrosilite crystal was synthesized is represented by the circle. (**b**) The $FeSiO_3$ phase diagram postulated as a result of this work (ignoring the presence of a second $C2/c$ stability field at high temperatures), showing the position of a $C2/c$ phase at high pressures, and uniting the results of Lindsley and Akimoto et al.

TABLE 1. Unit-cell parameters for $FeSiO_3$ and $MgSiO_3$

	a (Å)	b (Å)	c (Å)	β (°)	V (Å³)
$P2_1/c$ Fs; RT,P	9.7075(5)	9.0807(4)	5.2347(5)	108.46(1)	437.70(6)
C2/c Fs; 1.87 GPa	9.540(1)	8.996(3)	5.008(1)	103.01(1)	418.8(2)
C2/c Fs; 1050 °C	9.928(1)	9.179(1)	5.338(1)	110.20(1)	456.5(1)
C2/c Fs; Hd-like	9.73(1)	9.11(1)	5.23(1)	107.8(9)	441.4(8)
$P2_1/c$ En; RT,P	9.605(4)	8.814(3)	5.169(2)	108.34(4)	415.4(3)
C2/c En; 7.93 GPa	9.201(3)	8.621(1)	4.908(1)	101.50(3)	381.5(2)
C2/c En; 1100 °C	9.864(6)	8.954(4)	5.333(3)	110.03(4)	442.5(5)

Note: data for $P2_1/c$ and high-P Fs ($FeSiO_3$) and $P2_1/c$ and high-P En ($MgSiO_3$) are from our own experiments. High-T C2/c Fs data were taken from Sueno et al. (1984); high-T C2/c En data were taken from Smith (1969). Hd-like data were extrapolated from data across the CaFe-FeFe join (see text).

<0.8%. To check that the ferrosilite crystal was of a suitable quality for high-pressure X-ray diffraction, data were collected at ambient pressure and temperature with a glass-fiber mount before the crystal was transferred to a modified Merrill-Bassett type diamond-anvil cell (Hazen and Finger, 1982). A 4:1 methanol-ethanol mixture was used as the pressure medium, and the pressure was determined by using the R_1 laser-induced fluorescence from a small ruby chip included in the cell; the wavelength shifts were converted into pressures using the calibration of Mao et al. (1986), and the precision of these pressure measurements was estimated to be better than ±0.03 GPa (Angel et al., 1992b).

A Picker four-circle diffractometer equipped with a Mo X-ray tube (with $K\alpha$ radiation obtained by β filtering) was used throughout the course of the experiment. Unit cells were determined at each pressure by a vector least-squares fit (Ralph and Finger, 1982) to the positions of about 25 accessible reflections in the range $8° < 2\theta < 28°$, centered by the method of King and Finger (1979). All the unit cells displayed monoclinic symmetry within the experimental uncertainties, and cell parameters constrained to monoclinic symmetry are reported in Tables 1 and 2.[1]

To determine the nature of structural changes occurring, intensity data of all accessible reflections to 60° 2θ were collected, with ω scans of 1° total width and a step size of 0.025°, in a constant-precision mode to obtain $I/\sigma_I > 10$, subject to the restriction of a maximum counting time per step of 8 s. Standard reflections were collected every 200 min to check for drift of the diffractometer and intensity decrease. No significant or systematic variations in these reflections were observed during the course of any of the data collections. Integrated intensities were obtained from the step scans using a modified Lehmann-Larsen algorithm (Grant and Gabe, 1978), with the option to reset the backgrounds interactively and so exclude any diffuse background. Intensities were corrected for absorption by the diamond, Lorentz and polarization effects, and absorption by the crystal itself (typically, $\mu = 72\ cm^{-1}$). The reflections were averaged in Laue group $2/m$. The y coordinates of the high-pressure clinoferrosilite structure (from the first data collection) were poorly defined as a result of lack of resolution along **b***, which was caused by the orientation of the crystal within the diamond-anvil cell enforced by the crystal's cleavage. Consequently the crystal was unloaded from the diamond-anvil cell and remounted in such a way that the new orientation was approximately 90° from the initial orientation. The pressure was increased to 1.88 GPa (i.e., within 1 esd of the previous pressure), and a second data set was collected. Absorption corrections were made, and the individual data sets were averaged in Laue group $2/m$; then the two sets of intensity data were combined for the final structure refinement. Structure factors with $F > 6\sigma_F$ were refined using the RFINE90 program, a development version of the RFINE4 program (Finger and Prince, 1975), with reflections assigned weights of σ^{-2}, where σ was derived from counting and averaging statistics. Refinement parameters and averaging statistics for both sets of intensity data are given in Table 3.

RESULTS

The structure of the clinoferrosilite crystal with space group $P2_1/c$ was determined at room pressure, and positional parameters and bond lengths and angles are reported in Tables 4 and 5, respectively. All structural parameters are within 1 esd (combined) of those measured by Burnham (1966).

On compression to 1.43 GPa, the clinoferrosilite crystal exhibited $P2_1/c$ cell parameters, which are characterized by a relatively large β angle of ~108°. At these low pressures, there was no significant variation in the intensities of the $h + k = 2n + 1$ reflections that are present in the diffraction pattern of $P2_1/c$ clinoferrosilite. On increasing the pressure further to 1.75 GPa, these reflections disappeared from the diffraction pattern, and the unit-cell parameters underwent a discontinuous change; whereas a decreased by ~1.3%, c shortened by some 4%, and β was reduced by about 5° to a value of 103.07° (Figs. 2 and 3). The transition was accompanied by a 3% volume decrease, which indicates that the transition is first-order in character. On releasing the pressure from the crystal, the structure once again assumed the $P2_1/c$ clinoferrosilite structure, with its large value of β. Subse-

[1] A copy of Table 2 may be requested from the authors or ordered as Document AM-94-571 from the Business Office, Mineralogical Society of America, 1130 Seventeenth Street, NW, Suite 330, Washington, DC 20036, U.S.A. Please remit $5.00 in advance for the microfiche.

TABLE 3. Refinement parameters for $P2_1/c$ clinoferrosilite and high-pressure clinoferrosilite

Phase	$P2_1/c$ (1 atm)	$C2/c$ (1.87 GPa)	
Data set (for $C2/c$ phase, see text)		1	2
No. refl. before averaging	2046	570	348
No. obs., $I > 3\sigma_I$	1114	344	199
$R_{av.}$	0.040	0.038	0.036
R_u	0.081	0.055	
R_w	0.087	0.047	
G_{fit}	1.95	1.27	

quent cycles of raising and lowering the pressure around the transition have yielded a reversed bracket of 1.48–1.75 GPa and show that the transformation is reversible and that the high-pressure phase is nonquenchable.

From diffraction data collected from the crystal at 1.87 GPa, it was found that all reflections with $h + k =$ odd were absent, and, of the $h0l$ reflections, those with $l =$ odd were also unobserved. These systematic absences are indicative of space group $C2/c$ or Cc. An $N(z)$ test (Wilson, 1949) on the intensities of all accessible reflections indicated that they display the statistics expected from a centric structure. A structure refinement of the combined data set was therefore carried out in space group $C2/c$ using as initial coordinates those of the high-pressure $C2/c$ pyroxene $MgSiO_3$ (Angel et al., 1992a). Refined positional parameters, bond lengths, and angles are reported in Tables 4 and 5.

Using orientation matrices obtained from diffraction data collected from the clinoferrosilite crystal above and below the transition, the orientational relationship for the transformation of the low- to the high-P clinoferrosilite structures was calculated as

$$\begin{matrix} 1 & 0 & 0.16 \\ 0 & 1 & 0 \\ 0 & 0 & 1. \end{matrix}$$

Since this relationship between the high- and low-P structures consists of two independent components (i.e., that due to the crystallographic transition from the $P2_1/c$ to $C2/c$ phases and also a possible movement of the crystal within the diamond-anvil cell between experiments), the above matrix was calculated for several experimental reversals, giving the estimated uncertainties for each component of the matrix as ± 0.03. Within these limits, the crystallographic relationship between the $P2_1/c$ and high-P $C2/c$ phases of $FeSiO_3$ is identical to that calculated for $MgSiO_3$.

DISCUSSION

Nature of the $P2_1/c$ to high-P $C2/c$ transition in Mg and Fe end-member pyroxenes

The change in symmetry from $P2_1/c$ to $C2/c$ of the clinoferrosilite may be described by differences in the configuration of the silicate chains within the pyroxene framework, in a similar way to the $P2_1/c$–$C2/c$ transition

TABLE 4. Positional parameters for the $P2_1/c$ and high-pressure $C2/c$ $FeSiO_3$ phases

		$P2_1/c$ (1 atm)		$C2/c$
		A chain	B chain	(1.87 GPa)
Fe1	x	0.2512(3)		0.00
	y	0.6538(2)		0.9054(6)
	z	0.2262(5)		0.25
	B_{iso}	0.92(5)		0.38(6)
Fe2	x	0.2256(3)		0.00
	y	0.0145(3)		0.2721(4)
	z	0.2239(5)		0.25
	B_{iso}	1.13(5)		0.28(7)
Si	x	0.0454(5)	0.5531(5)	0.2988(4)
	y	0.3384(5)	0.8334(5)	0.0882(8)
	z	0.2915(9)	0.2431(9)	0.2225(6)
	B_{iso}	0.64(7)	0.77(7)	0.05(5)
O1	x	0.871(1)	0.379(1)	0.126(1)
	y	0.338(1)	0.837(1)	0.095(2)
	z	0.178(2)	0.137(2)	0.154(2)
	B_{iso}	0.62(17)	0.59(16)	0.30(11)*
O2	x	0.125(1)	0.633(1)	0.377(1)
	y	0.496(1)	0.981(1)	0.233(2)
	z	0.335(2)	0.387(3)	0.373(2)
	B_{iso}	0.70(17)	1.17(21)	0.30(11)*
O3	x	0.106(1)	0.608(1)	0.352(1)
	y	0.266(1)	0.702(1)	0.053(1)
	z	0.597(3)	0.470(2)	0.934(2)
	B_{iso}	1.45(21)	1.60(22)	0.30(11)*

* These isotropic displacement factors were constrained to be identical during the structure refinement because of poor data coverage along **y***.

in the $MgSiO_3$ end-member (Angel et al., 1992a). All pyroxene polymorphs consist of chains of corner-sharing silicate tetrahedra that crosslink, by shared O atoms, parallel bands of octahedrally coordinated cations. These tetrahedral chains may be rotated in two directions from the fully extended position, denoted O and S rotations (Thompson, 1970). The differences between these rotations are most clearly defined in terms of ideal structures with fully rotated chains (Fig. 4), with the O configuration having a chain extension angle O3-O3-O3 of 120°, and a resulting structure based on a cubic close-packed arrangement of O atoms (with a tetrahedral to octahedral edge ratio of 1:1). Hexagonal close-packing of the O atoms produces a structure with S-rotated chains whose chain extension angle is 240° by convention (Cameron and Papike, 1980). In an O-rotated tetrahedral chain, the basal triangular faces of the tetrahedra [i.e., those approximately parallel to (100)] have an orientation opposite to the triangular faces of the octahedral strip to which they are linked by the apical O1 atoms (Fig. 4a). In an S-rotated chain, however, these triangular faces have the same orientation (Fig. 4b). Both situations represent extreme rotations; in practice, the chain extension angle is never less than about 130° and is usually in the range 160–175° (Cameron and Papike, 1980). Fully extended chains in an ideal structure have an extension angle O3-O3-O3 of 180°; this structure is only possible if the tetrahedral to octahedral edge ratio is $\sqrt{3}$:2 (Fig. 4c). Note that the tetrahedral to octahedral edge ratio increases with the rotation of the silicate chains away from the fully extended position (in either the O or S direction), so that increased

TABLE 5. Bond lengths and angles for four monoclinic $FeSiO_3$ polymorphs

	C2/c		Fictive Hd-like C2/c	P2₁/c at RT, 1 atm	
	1.87 GPa	1050 °C*		A chain	B chain
Fe1-O1	2.20(2)	2.28(2)	2.07(1)	2.08(1)	2.09(1)
Fe1-O1	2.109(8)	2.104(8)	2.22(1)	2.20(1)	2.20(1)
Fe1-O2	2.12(1)	2.15(1)	2.105(9)	2.11(1)	2.13(1)
⟨Fe1-O⟩	2.14(1)	2.18(2)	2.13(1)	2.13(1)	
Fe1 *V*	13.0(1)	13.5(1)	12.8(1)	12.8(1)	
Fe1 quad. el.	1.0083	1.0097	1.0088	1.0091	
Fe2-O1	2.12(2)	2.16(2)	2.10(1)	2.16(1)	2.13(1)
Fe2-O2	1.990(9)	2.016(9)	2.005(5)	2.04(1)	1.99(1)
Fe2-O3	2.43(1)	2.72(1)	2.91(3)	2.45(1)	2.57(1)
7/8th Fe2-O		3.19(2)	3.00(3)		
⟨Fe2-O⟩ of 6	2.18(1)	2.30(2)	2.33(1)	2.22(1)	
Fe2 *V*	13.6(1)	25.3(2)	24.0(2)	13.5(1)	
Fe2 quad. el.	1.0182			1.0648	
Si-O1	1.61(1)	1.60(1)	1.625(5)	1.62(1)	1.61(1)
Si-O2	1.60(1)	1.61(1)	1.605(1)	1.58(1)	1.59(1)
Si-O3	1.67(1)	1.65(1)	1.64(1)	1.63(1)	1.65(1)
Si-O3	1.66(1)	1.67(1)	1.641(1)	1.65(1)	1.69(1)
⟨Si-O⟩	1.63(1)	1.63(1)	1.631(5)	1.62(1)	1.64(1)
Si *V*	2.22(2)	2.22(2)	2.215(8)	2.17(1)	2.24(1)
Si quad. el.	1.0024	1.0047	1.0034	1.0063	1.0049
O3-Si-O3	107.4(0.5)	107.6(0.7)	108.7(0.5)	106.7(0.4)	110.8(0.4)
O3-O3-O3	138.4(0.9)	169.5(0.8)	156.3(0.4)	192.9(0.9)	144.1(0.9)

Note: the bond lengths and angles of the Hd-like *C2/c* ferrosilite were calculated in two ways—the first method involved the extrapolation of unit-cell parameters and atomic coordinates across the hedenbergite-ferrosilite join (see text) to form a fictive structure, from which bond lengths and angles were calculated. The other method was simply to extrapolate the bond lenths and angles across the join, using the published lengths and angles of Cameron et al. (1973) and Ohashi et al. (1975). The estimated standard deviations reported for the Hd-like *C2/c* phase represent the differences between the results from the two methods.

* Sueno et al. (1984).

chain rotation leads to relatively smaller octahedral cation sites (Cameron and Papike, 1980). For this last reason, Pannhorst (1979, 1981) chose to distinguish pyroxenes on the basis of the stacking sequence of nearly straight and kinked chains.

The structure of clinoferrosilite with space group $P2_1/c$ consists of two symmetrically distinct silicate chains, which are rotated in different directions. The A chain is S-rotated and is more extended with smaller tetrahedra than the B chain, which is O-rotated and considerably kinked. The edge sharing of the tetrahedra and M2 site that results from the S rotation of the A chain makes the M2 octahedral site extremely distorted. The chain extension angles of the $P2_1/c$ clinoferrosilite show very large rotations from 180°, indicating that the structure is near its stability limit. Since the SiO_4 tetrahedra are relatively incompressible at low pressures, increasing the pressure tends to compress the FeO_6 octahedra differentially, thus requiring further rotation of the tetrahedral chains from the straight configuration to stabilize the structure. Since the chains are already as kinked as they can readily become, the structure undergoes a major reconfiguration of the silicate chains between 1.43 and 1.75 GPa. Above the transition pressure, the A chain becomes O-rotated (i.e., kinked in the opposite sense from the fully extended position, relative to its kinking in the low-pressure structure) and becomes geometrically equivalent to the B chain. Note that this chain rotation also involves the breaking of the bonds between each O3 atom of the A chain and the M2 Fe atoms on one side of the chain and the formation of new bonds between the O3 and M2 sites on the other side (schematically shown in Fig. 4a, 4b). As a result, the tetrahedra in the A chain no longer share edges with the M2 sites, and this allows these octahedra to become significantly smaller. The unit-cell volume of the pyroxene is reduced by some 12 Å^3 by the transformation to a pyroxene with a small chain extension angle of 138.4°. Under Pannhorst's (1979) description, the transformation involves a change in stacking sequence from M + SS − M + KK − M in the $P2_1/c$ phase to M + KK − M + KK − M for the high-pressure $C2/c$ structure, where S denotes a layer of relatively straight tetrahedral chains, K a layer of kinked chains, and M the octahedral layer.

The nature of this low- to high-P clino transformation is very similar to that occurring above 7 GPa in clinoenstatite (Angel et al., 1992a). In both the $FeSiO_3$ and the $MgSiO_3$ end-member compositions, the transition is accompanied by a 3% volume decrease and a decrease of about 6° in β (Figs. 2 and 3). However, the magnitude of the hysteresis loop between the high-P ($C2/c$) and low-P ($P2_1/c$) structures is much greater in the $MgSiO_3$ end-member (about 2.6 GPa) than in the ferrosilite, which our reversals demonstrate must be $<0.27 \pm 0.05$ GPa.

From a study of many pyroxenes of various compositions and all space groups, Cameron and Papike (1980) determined the relationships between ionic cation radius for the octahedral sites and several internal bond lengths and angles. They showed that, as the radius of the M2 cation increases, the average Si-O bond lengths also increase. For a change in M2 cation radius from that of Mg^{2+} to that of Fe^{2+}, average Si-O bond lengths in the $C2/c$ structure are predicted to increase by about 0.005

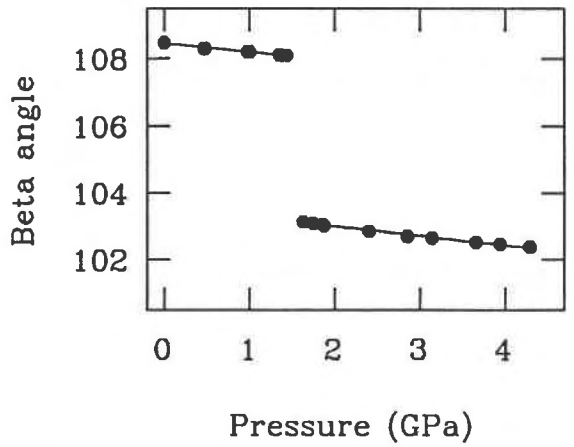

Fig. 2. The variation of β with pressure of the clinoferrosilite ($FeSiO_3$), showing a distinct discontinuity of some 5° at the transition from $P2_1/c$ to $C2/c$. The uncertainties in the measurements of β and the pressure are considerably less than the size of the symbols used.

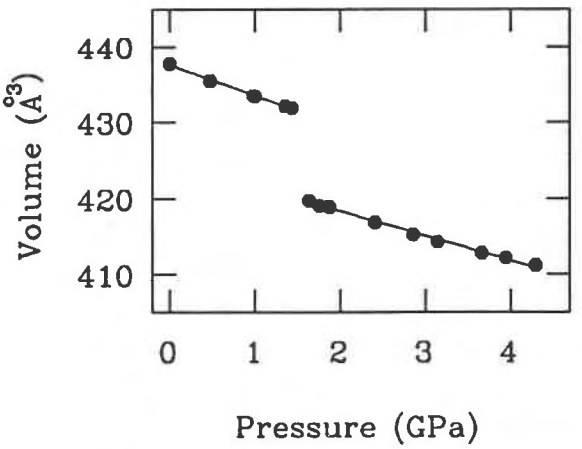

Fig. 3. The variation of unit-cell volume of the clinoferrosilite ($FeSiO_3$) with pressure, showing a discontinuous jump of about 12 Å^3 at the position of the $P2_1/c$ to $C2/c$ transition. The uncertainties in the measurements of both the volume of the unit cell and the pressure are considerably less than the size of the symbols used.

Å and the average M2-O bond lengths by about 0.009 Å; the O3-O3-O3 chain angle is predicted to decrease by up to about 5°. Our data for the high-P $C2/c$ polymorph of both end-member compositions show that both Si-O and M2-O bond lengths behave as expected, whereas the O3-O3-O3 chain extension angle appears to increase by some 3° as Mg is replaced by Fe in the M1 and M2 sites. A similar examination of the behavior of the $P2_1/c$ polymorphs (using the trends determined by Cameron and Papike, 1980) revealed that the average Si-O bond length in both silicate chains shortens as the radius of the octahedral cation increases, whereas the average M2-O bond length increases, as expected. Both A and B chains are predicted to rotate toward the straight position by approximately 7° as Fe replaces Mg in the cation sites; within the experimental uncertainties, this was found to be the case. From these trends it may be assumed that changing the composition along the Mg,Fe join has few unexpected structural consequences—most of the bond lengths and angles of the monoclinic phases can be successfully predicted, and although the pressure of the low-P ($P2_1/c$)–high-P ($C2/c$) transition varies with composition, the nature of the transformation does not.

The relationship between three $C2/c$ structures

$FeSiO_3$. The structures of two other polymorphs of clinoferrosilite with space group $C2/c$ may be considered. A high-temperature phase, formed by heating a $P2_1/c$ clinoferrosilite crystal to 1050 °C, was reported by Sueno et al. (1984). Secondly, a high-Ca, or hedenbergite-like (Hd-like), structure can be postulated as a fictive $FeSiO_3$ end-member of the hedenbergite-ferrosilite solid-solution. We have modeled the structure of this Hd-like phase by extrapolating the published unit-cell parameters and atomic coordinates for pyroxenes along the hedenbergite-ferrosilite join with space group $C2/c$ and intermediate Ca contents (Cameron et al., 1973; Ohashi et al., 1975) to predict those for a hypothetical hedenbergite-like $FeSiO_3$ composition. From the atomic positions calculated in this way (Table 6), the complete clinopyroxene structure was generated, and bond lengths, angles, and polyhedral volumes were derived (Table 5). Unit-cell parameters for all the monoclinic phases of $FeSiO_3$ that we discuss here are given in Table 1.

The most striking difference between these three $C2/c$ polymorphs is the unusually small value of β in the high-P structure. This angle of about 103° is more than 7° less than that observed in the high-T phase at 1050 °C (Sueno et al., 1984) and nearly 5° less than that calculated for the Hd-like phase. There is evidence to show that β may increase as much as 3° in a temperature rise of 1000 °C (Smyth, 1974), in which case both the high-T and the fictive Hd-like phases have a value for β at room temperature of about 108°. The extrapolated room-pressure unit-cell volume of the high-P phase is more than 8% less than the volume of the high-T phase; only about 1% of this difference arises from the thermal expansion of the pyroxene at elevated temperatures. The unit-cell volume of the high-P form is also 5% less than that of the Hd-like phase, thus showing that the volumes of both the high-T and the fictive Hd-like polymorphs are very similar at ambient temperature and pressure. The a, b, and c cell parameters of the high-P $C2/c$ phase are all significantly shorter than the corresponding cell parameters of either the high-T or fictive Hd-like polymorphs, the cell parameters of these latter two phases (those of the high-T form having been corrected for thermal expansion) being of a similar magnitude. These comparisons seem to suggest that, at a superficial level, the structures of the high-T and Hd-like phases are similar, and both are distinct from the $C2/c$ phase found at high pressures.

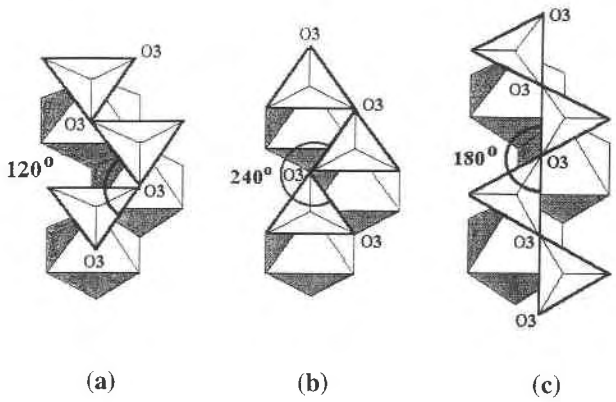

Fig. 4. Completely (a) O- and (b) S-rotated and (c) extended tetrahedral chain configurations for an ideal pyroxene structure (after Cameron and Papike, 1980). The rotations are defined by the relative orientations of the basal face of the tetrahedra [i.e., that approximately parallel to (100)] and the uppermost face of the M1 octahedra to which they are linked.

The O3-O3-O3 chain extension angle of each phase (Table 5) is very important for characterizing the differences between the monoclinic pyroxene polymorphs. There is only one symmetrically distinct silicate chain in the *C2/c* structure, which is O-rotated to differing degrees in all the polymorphs (Table 5). It is slightly more than 10° from the fully extended position in the high-*T* phase [with stacking sequence M + SS − M + SS − M under Pannhorst's classification (1979)], allowing the M2 sites to become very large and highly distorted from an ideal octahedron. In the fictive Hd-like phase, the chain extension angle is approximately 156°, and the Fe in the M2 site occupies a distorted eightfold-coordinated polyhedron with very large volume. Only the high-*P* clinoferrosilite exhibits a remarkably small chain extension angle, some 20° less than the Hd-like phase, and more than 30° less than the extended high-*T* silicate chains. Extrapolation of this high-*T* extension to ambient temperature (by noting the effect of temperature on *C2/c* pyroxenes such as diopside and hedenbergite: Cameron et al., 1973) merely reduces the chain extension angle by about 3°. As far as the chain extension angles are concerned, the Hd-like structure is therefore intermediate between that of the high-*P* and high-*T* structures but is much nearer to that of the high-*T* structure (Fig. 5). The average Si-O bond lengths in all three phases are identical to within 1 esd (combined), though the tetrahedra are somewhat more distorted at high temperature. The M1 site does not differ significantly in either shape or size between the three *C2/c* phases, although it is approximately 5% larger in the high-*T* structure. Thermal expansion is likely to contribute up to 1.5% of this difference, and the remainder may be accounted for by the experimental uncertainties.

The most significant variation in size and shape of the cation sites in the high-*P*, high-*T*, and fictive Hd-like structures occurs at the M2 site, which is connected to the silicate chains by the long M2-O3 bonds; kinking of the chains away from the extended position inevitably leads to smaller and more regular M2 sites. Since the silicate chains are highly kinked at high pressure (with an O3-O3-O3 angle of 138.4° at 1.87 GPa), the M2 octahedron is indeed fairly regular but the M2 site becomes almost eightfold-coordinated and very distorted at high temperatures, with a dramatic increase in polyhedral volume (Fig. 5). Sueno et al. (1984) calculated the volume of this eightfold-coordinated polyhedron to be approximately 25.25 Å^3, a volume that is comparable with volumes of the M2 polyhedra found in Na- and Ca-containing pyroxenes (Cameron et al., 1973). The M2 site in the Hd-like phase is also a distorted eightfold-coordinated polyhedron, with a similarly large volume to that at high temperature. It is likely that at high temperatures the Fe atoms vibrate more rapidly in the expanded and distorted M2 polyhedra, causing them to resemble the eightfold-coordinated polyhedra found in Ca-containing pyroxenes and also in the fictive Hd-like $FeSiO_3$ structure.

Table 6. Calculated positional parameters for the Hd-like *C2/c* $FeSiO_3$ phase

	x	*y*	*z*
Fe1	0.0	0.901	0.25
Fe2	0.0	0.263	0.25
Si	0.296	0.085	0.252
O1	0.124	0.090	0.159
O2	0.375	0.240	0.362
O3	0.359	0.031	0.045

$MgSiO_3$. Since the Ca-poor component of pyroxene in the upper mantle is likely to have the approximate composition $Mg_{0.85}Fe_{0.15}SiO_3$, it would be of use to carry out the same comparisons with three Mg-rich *C2/c* pyroxenes. The structures of the low-*P* ($P2_1/c$) and high-*P* structures of clinoenstatite ($MgSiO_3$) have already been determined (Ohashi, 1984; Angel et al., 1992a), but no published data for a pure $MgSiO_3$ *C2/c* form stable at high temperatures are available. However, there is much experimental evidence for the existence of such a phase (e.g., Perrotta and Stephenson, 1965; Smith, 1969; Shimobayashi and Kitamura, 1991), with the temperature of the metastable low-*T* ($P2_1/c$)–high-*T* (*C2/c*) transition increasing as the Mg content is increased across the $FeSiO_3$-$MgSiO_3$ join (Prewitt et al., 1971). The only published structure of a Mg-containing *C2/c* pyroxene at high temperature is that of Smyth (1974), who determined the structure for the composition $Mg_{0.32}Fe_{0.68}SiO_3$. We have therefore estimated the structure of a high-*T* *C2/c* $MgSiO_3$ phase by extrapolation along the Mg-Fe join. A model of a high-Ca structure was formed by extrapolation along the diopside-enstatite join to form a diopside-like (Di-like) structure, which is less well defined at the Mg end of the Mg,Fe solid solution because of inconsistencies in the published structural data for pyroxenes of intermediate compositions. Unit-cell parameters for the Mg-containing *C2/c* clinopyroxenes are given in Table 1.

Comparisons of these monoclinic polymorphs of $MgSiO_3$ pyroxene show that the differences between the

high-*P*, high-*T*, and Di-like polymorphs are very similar to those seen in the ferrosilite end-member. As with the high-*P* ferrosilite phase, the high-*P* *C2/c* phase of $MgSiO_3$ may be distinguished by its low β angle of 101.5° and its extremely kinked tetrahedral chain (Angel et al., 1992a). This chain extension angle of 133.4° is the smallest ever reported for any pyroxene and is significantly smaller than the B chain of $P2_1/c$ clinoenstatite (138.3°). The high-*T* *C2/c* structure of $Mg_{0.32}Fe_{0.68}FeSiO_3$ (Smyth, 1974), on the other hand, has extremely extended silicate chains, with a chain extension angle only 7° from the ideal straight-chain configuration. This substantial extension of the silicate chain implies that the M2 sites are both large, highly distorted, and irregular—a structural determination (Smyth, 1974) of this pyroxene at 825 °C shows that this is indeed the case. The fictive Di-like phase of $MgSiO_3$ also has an eightfold-coordinated M2 site, though it is more regular than the high-*T* M2 site but has a similar volume. The silicate chains in the Di-like structure are thus less extended than the high-*T* chains but significantly more extended than those seen at high pressures.

The relationship between the *C2/c* and orthorhombic (*Pbca*) polymorphs

It has often been assumed for geochemical experiments that the stable upper-mantle phase of Ca-poor pyroxene is the orthorhombic polymorph (with space group *Pbca*) rather than this newly characterized monoclinic phase with space group *C2/c*, which for the $FeSiO_3$ end-member composition becomes stable at a depth of about 50–60 km. It is useful, therefore, to compare the structures of these two phases, in particular the size and distortion of the M2 sites, to predict the effect that the orthorhombic to *C2/c* phase transition will have on the trace element partitioning behavior of the pyroxene. Although there is no significant difference (within the experimental uncertainties) in shape or size of the M1 sites in the *Pbca* phase (data for this orthorhombic phase were taken from experiments currently in progress) and the *C2/c* phase stable at high *P*, the M2 site is somewhat less distorted in the high-*P* *C2/c* polymorph. In both phases, this M2 cation is octahedrally coordinated, with identical average M2-O bond length [within 1 esd (combined)] and polyhedral volume. Within the experimental uncertainties, the tetrahedral sites in both pyroxene polymorphs discussed here are identical in both their average Si-O bond lengths and polyhedral volumes. These structural similarities of the high-*P* *C2/c* and *Pbca* polymorphs also apply to the $MgSiO_3$ end-member of the ferrosilite-enstatite solid-solution, with the M2 cation site being less distorted in the

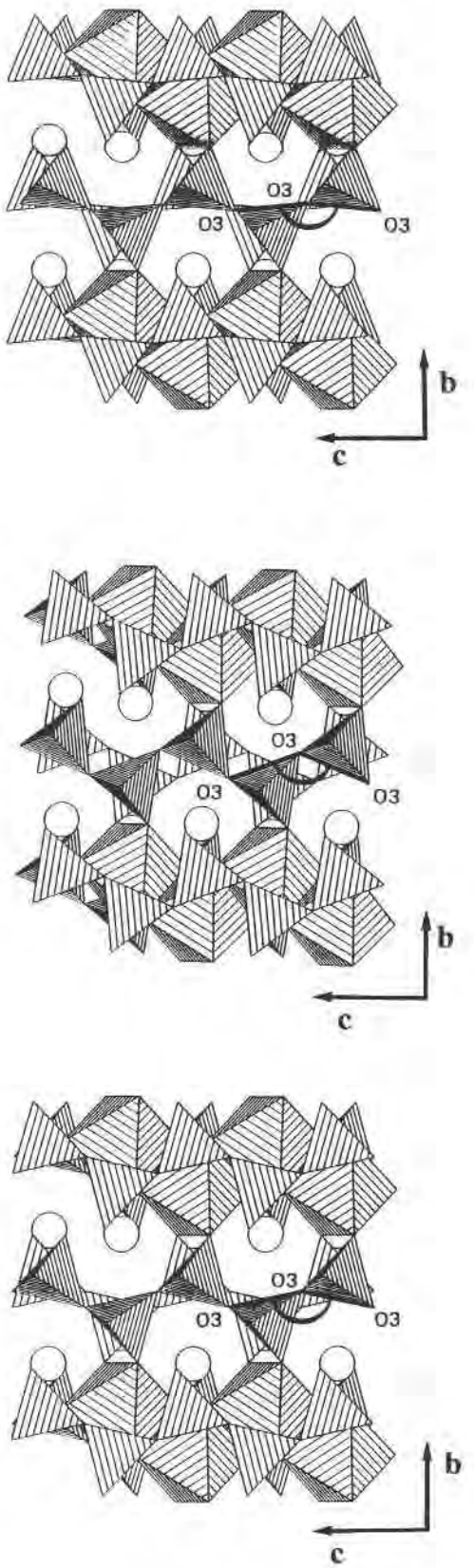

→

Fig. 5. The structures of (**a**) the high-temperature, (**b**) the high-pressure, and (**c**) the high-Ca (or Hd-like) *C2/c* phases of $FeSiO_3$ projected onto (100). The tetrahedral and M1 sites are shown as shaded tetrahedra and octahedra, respectively, and the M2 sites are drawn as circles. Note the variation of the chain extension angle (O3-O3-O3) between the three structures.

high-P $C2/c$ structure and the geometries of both the tetrahedral and M1 octahedral sites being identical within experimental uncertainties.

Conclusions

Our reversal of the $P2_1/c$-$C2/c$ phase boundary at room temperature between 1.48 and 1.75 GPa, together with the recovery of clinoferrosilite from pressures exceeding 5 GPa (Akimoto et al., 1965) demonstrates that the $C2/c$ polymorph is the stable phase of $FeSiO_3$ at high pressure. The transformation is nonquenchable, so that the $C2/c$ polymorph reverts to the $P2_1/c$ clinoferrosilite form on pressure release. This observation allows us to reconcile the experimental results of Lindsley (1965) and Akimoto et al. (1965). Lindsley's experiments are now seen to be reversals of the $P2_1/c$-ortho phase boundary. The synthesis experiments (and one reversal) of Akimoto et al. approximated the position of a phase boundary between ortho and $C2/c$ ferrosilite, products from the $C2/c$ side of the boundary quenching to $P2_1/c$ clinoferrosilite. The overall topology of the phase diagram deduced from these experiments and our reversal of the $P2_1/c$-$C2/c$ transition is shown in Figure 1b and is very similar to that of $MgSiO_3$ (Angel et al., 1992a; Angel and Hugh-Jones, 1994), although the $FeSiO_3$ phase boundaries and the triple point are shifted to lower pressures.

The stable form of both pure enstatite and pure ferrosilite at the temperatures and pressures of the Earth's upper mantle is thus the high-pressure $C2/c$ pyroxene polymorph. It is reasonable to assume that the transformation of orthoenstatite to the high-P $C2/c$ phase also occurs for Ca-poor orthopyroxene compositions close to the $MgSiO_3$-$FeSiO_3$ join. Although this transformation should have significant effects on the thermodynamic parameters of the pyroxene (Angel and Hugh-Jones, 1994), the comparison of the structures of the $C2/c$ and *Pbca* polymorphs of both $FeSiO_3$ and $MgSiO_3$ shows that the sizes and distortions of the cation sites are very similar. We therefore do not expect that the transformation at high pressures of orthopyroxene to $C2/c$ pyroxene should have any great effect either on the solid solution limits of the pyroxene phase or upon its ability to take up trace elements. In particular, by the use of fictive high-Ca end-members, we have shown that the structures of the high-pressure $C2/c$ phases are substantially different from those of $C2/c$ pyroxenes containing Ca. We therefore expect the miscibility gaps between the orthopyroxenes $MgSiO_3$ and $FeSiO_3$ and their corresponding solid solutions, $(Ca,Mg)MgSi_2O_6$ and $(Ca,Fe)FeSi_2O_6$, also occur between the $C2/c$ phases of $MgSiO_3$ and $FeSiO_3$ and these solid solutions.

There is also substantial evidence for the stability of a second phase with $C2/c$ symmetry at ambient pressure and temperatures exceeding about 1000 °C in both $MgSiO_3$ and $FeSiO_3$ compositions (for example, Perrotta and Stephenson, 1965; Smith, 1969; Sueno et al., 1984). Our detailed comparisons of the high-pressure and high-temperature $C2/c$ structures have shown that they are very different, even allowing for the converse effects of temperature and pressure. For example, it is unlikely that the effect of temperature on a $C2/c$ pyroxene equilibrated at a high pressure would alter β or the chain extension angle uniformly to be characteristic of the high-temperature $C2/c$ pyroxene. The phase diagram for the $MgSiO_3$-$FeSiO_3$ system therefore contains two structurally distinct $C2/c$ phases, whose stability fields may meet at a kind of crossover transition at very high pressures and temperatures (although such a transition would probably be metastable with respect to orthopyroxene).

At ambient temperature, pyroxenes containing $<\sim 15\%$ Ca in the $Ca(Mg,Fe)SiO_3$-$(Mg,Fe)SiO_3$ solid solution range are stable as a low-symmetry $P2_1/c$ structure (Ohashi et al., 1975); as the temperature is increased, a high-T, high-symmetry $C2/c$ structure is stabilized. Since the structures of the high-temperature and high-Ca $C2/c$ phases are similar in the $MgSiO_3$ and $FeSiO_3$ end-members (especially in terms of the sizes and distortions of their M1 and M2 cation sites), the structural trends across the hedenbergite-ferrosilite and diopside-enstatite joins appear to be continuous at some high temperature [for example, that of the $P2_1/c$ to $C2/c$ transition in the equivalent Ca-free $(Mg,Fe)SiO_3$ end-member]. Any variation in the structure of this high-T $C2/c$ phase as the composition changes from Ca-rich to Ca-poor would be caused solely by the substitution of Fe for Ca in the M1 and M2 sites; the resulting structure of the pyroxene of intermediate Ca content may be postulated using the trends of Cameron and Papike (1980).

Acknowledgments

We would like to thank F. Liebau and two anonymous reviewers for their comments on this manuscript and also C. McCammon for her Mössbauer experiments on the clinoferrosilite sample. In addition, D.A.H.-J. would like to thank T. Sharp and A. Hogrefe for their assistance with the TEM analyses. This work was supported by an NERC studentship, no. GT4/4/92/223, to D.A.H.-J., a Royal Society University Research Fellowship, and an NERC research grant GR9/945 to R.J.A. This is contribution no. 36 from the joint Research School of Geological and Geophysical Sciences, University College London.

References cited

Akaogi, M., and Akimoto, S. (1977) Pyroxene-garnet solid-solution equilibria in the system $Mg_4Si_4O_{12}$-$Mg_3Al_2Si_3O_{12}$ and $Fe_4Si_4O_{12}$-$Fe_4Al_2Si_3O_{12}$ at high pressures and temperatures. Physics of the Earth and Planetary Interiors, 15, 90–106.

Akimoto, S., Katsura, T., Syono, Y., Fujisawa, H., and Komada, E. (1965) Polymorphic transition of pyroxenes $FeSiO_3$ and $CoSiO_3$ at high pressures and temperatures. Journal of Geophysical Research, 70, 5269–5278.

Angel, R.J., and Hugh-Jones, D.A. (1994) Equations of state and thermodynamic properties of enstatite pyroxenes. Journal of Geophysical Research, in press.

Angel, R.J., Chopelas, A., and Ross, N.L. (1992a) Stability of high-density clinoenstatite at upper-mantle pressures. Nature, 358, 322–324.

Angel, R.J., Ross, N.L., Wood, I.G., and Woods, P.A. (1992b) Single-crystal X-ray diffraction at high pressures with diamond anvil cells. Phase Transitions, 39, 13–32.

Burnham, C.W. (1966) Ferrosilite. Carnegie Institution of Washington Year Book, 65, 285–290.

Cameron, M., and Papike, J.J. (1980) Crystal chemistry of silicate pyroxenes. Mineralogical Society of America Reviews in Mineralogy, 7, 5–92.

Cameron, M., Sueno, S., Prewitt, C.W., and Papike, J.J. (1973) High-temperature crystal chemistry of acmite, diopside, hedenbergite, jadeite, spodumene, and ureyite. American Mineralogist, 58, 594–618.

Finger, L.W., and Prince, E. (1975) A system of Fortran IV computer programs for crystal structure computations. U.S. National Bureau of Standards Technical Note, 854, 128 p.

Gasparik, T. (1990) A thermodynamic model for the enstatite-diopside join. American Mineralogist, 75, 1080–1091.

Grant, D.F., and Gabe, E.J. (1978) The analysis of single-crystal Bragg reflections from profile measurements. Journal of Applied Crystallography, 11, 114–120.

Hazen, R.M., and Finger, L.W. (1982) Comparative crystal chemistry, p. 25–38. Wiley, New York.

Herzberg, C., and Gasparik, T. (1991) Garnet and pyroxenes in the mantle: A test of the majorite fractionation hypothesis. Journal of Geophysical Research, 96, 16263–16274.

Kanzaki, M. (1991) Ortho/clinoenstatite transition. Physics and Chemistry of Minerals, 17, 726–730.

King, H., and Finger, L.W. (1979) Diffracted beam crystal centering and its application to high-pressure crystallography. Journal of Applied Crystallography, 12, 374–378.

Lindsley, D.H. (1965) Ferrosilite. Carnegie Institution of Washington Year Book, 65, 148–149.

Mao, H.K., Xu, J., and Bell, P.M. (1986) Calibration of the ruby pressure gauge to 800 kbar under quasi-hydrostatic conditions. Journal of Geophysical Research, 91, 4673–4676.

Ohashi, Y. (1984) Polysynthetically twinned structures of enstatite and wollastonite. Physics and Chemistry of Minerals, 10, 217–229.

Ohashi, Y., Burnham, C.W., and Finger, L.W. (1975) The effect of Ca-Fe substitution on the clinopyroxene crystal structure. American Mineralogist, 60, 423–434.

Pacalo, R.E.G., and Gasparik, T. (1990) Reversals of the orthoenstatite-clinoenstatite transition at high pressures and high temperatures. Journal of Geophysical Research, 95, 15853–15858.

Pannhorst, W. (1979) Structural relationships between pyroxenes. Neues Jahrbuch für Mineralogie Abhandlungen, 135, 1–17.

——— (1981) Comparison between topological classifications of pyroxenes. Neues Jahrbuch für Mineralogie Abhandlungen, 143, 1–14.

Perrotta, A.J., and Stephenson, D.A. (1965) Clinoenstatite: High-low inversion. Science, 148, 1090–1091.

Prewitt, C.T., Brown, G.E., and Papike, J.J. (1971) Apollo 12 clinopyroxenes: High temperature X-ray diffraction studies. Proceedings of the Lunar Science Conference, 2, 59–68.

Ralph, R.L., and Finger, L.W. (1982) A computer program for refinement of crystal orientation matrix and lattice constants from diffractometer data with lattice symmetry constraints. Journal of Applied Crystallography, 15, 537–539.

Ringwood, A.E. (1975) Composition and petrology of the Earth's mantle, p. 74–122. McGraw-Hill, New York.

Shimobayashi, N., and Kitamura, M. (1991) Phase transition in Ca-poor clinopyroxenes. Physics and Chemistry of Minerals, 18, 153–160.

Smith, J.V. (1969) Magnesium pyroxenes at high temperature: Inversion in clinoenstatite. Nature, 222, 256–257.

Smyth, J.R. (1974) The high temperature crystal chemistry of clinohypersthene. American Mineralogist, 59, 1069–1082.

Sueno, S., Kimata, M., and Prewitt, C.W. (1984) The crystal structure of high clinoferrosilite. American Mineralogist, 69, 264–269.

Thompson, J.B., Jr. (1970) Geometrical possibilities for amphibole structures: Model biopyriboles. American Mineralogist, 55, 292–293.

Wilson, A.J.C. (1949) The probability distribution of X-ray intensities. Acta Crystallographica, 2, 318–321.

Woodland, A.B., and O'Neill, H.St.C. (1993) Synthesis and stability of $Fe_3^{2+}Fe_2^{3+}Si_3O_{12}$ garnet and phase transitions with $Fe_3Al_2Si_3O_{12}$-$Fe_3^{2+}Fe_2^{3+}Si_3O_{12}$ solutions. American Mineralogist, 78, 1000–1013.

Yamamoto, K., and Akimoto, S. (1977) The system MgO-SiO_2-H_2O at high pressures and temperatures: Stability field for hydroxyl-chondrodite, hydroxyl-clinohumite and 10 Å-phase. American Journal of Science, 277, 288–312.

Manuscript received January 25, 1994
Manuscript accepted June 24, 1994